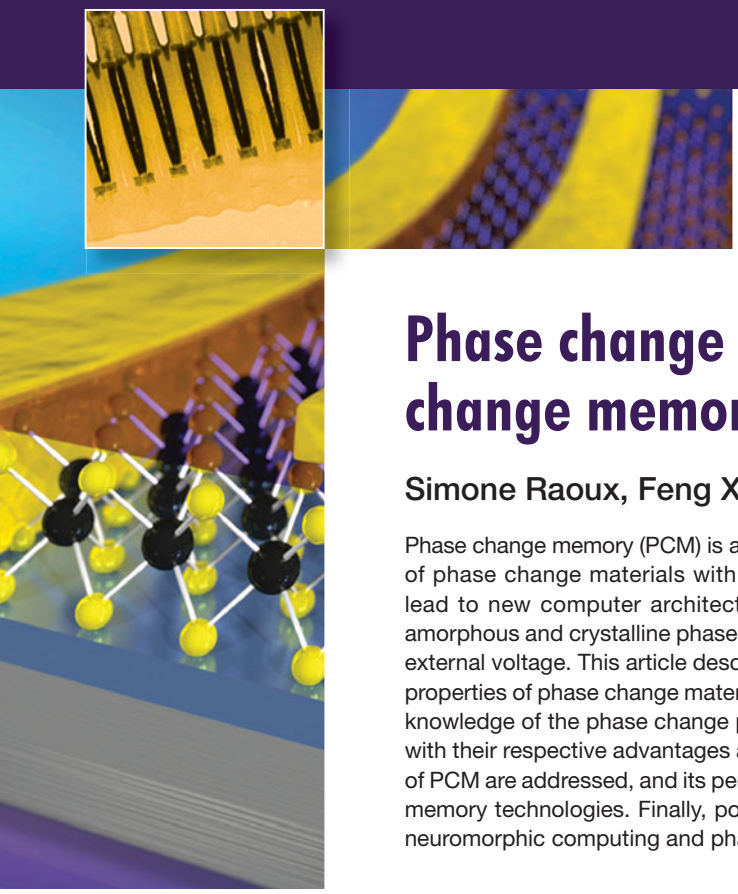


Phase change materials and phase change memory

Simone Raoux, Feng Xiong, Matthias Wuttig, and Eric Pop

Phase change memory (PCM) is an emerging technology that combines the unique properties of phase change materials with the potential for novel memory devices, which can help lead to new computer architectures. Phase change materials store information in their amorphous and crystalline phases, which can be reversibly switched by the application of an external voltage. This article describes the advantages and challenges of PCM. The physical properties of phase change materials that enable data storage are described, and our current knowledge of the phase change processes is summarized. Various designs of PCM devices with their respective advantages and integration challenges are presented. The scaling limits of PCM are addressed, and its performance is compared to competing existing and emerging memory technologies. Finally, potential new applications of phase change devices such as neuromorphic computing and phase change logic are outlined.

Introduction

Novel information storage concepts have been continuously developed throughout history, from cave paintings to printing, from phonographs to magnetic tape, dynamic random access memory (DRAM), compact disks (CDs), and flash memory, just to name a few. Over the last four decades, silicon technology has enabled data storage through charge retention on metal-oxide-silicon (MOS) capacitive structures. However, as silicon devices are scaled toward (sub-) 10 nm dimensions, minute capacitors become leaky by simple quantum mechanical considerations, and the memory storage density appears to plateau. Novel information storage concepts are under development that include storing data in the direction of the magnetic orientation (magnetic RAM,[1] spin torque transfer RAM,[2] racetrack RAM[3]), in the electric polarization of a ferroelectric material (ferroelectric RAM[4]), in the resistance of a memory device (resistive RAM,[5] memristor,[6] conducting bridge RAM,[7] carbon nanotube memory[8,9]), or in the resistance of the storage media itself (phase change RAM[10]). Phase change materials store information in their amorphous and crystalline phases, which can be reversibly switched by the application of an external voltage. In this article, we describe the properties of phase change materials and their application to phase change memory (PCM).

Properties of phase change materials

Phase change materials exist in an amorphous and one or sometimes several crystalline phases, and they can be rapidly and repeatedly switched between these phases. The switching is typically induced by heating through optical pulses or electrical (Joule) heating. The optical and electronic properties can vary significantly between the amorphous and crystalline phases, and this combination of optical and electrical contrast and repeated switching allows data storage. This effect was initially uncovered in 1968,[11] but it took the breakthrough discovery[12] of fast (i.e., nanosecond time scale) switching materials along the pseudo-binary line between GeTe and Sb_2Te_3, notably the most studied and utilized $Ge_2Sb_2Te_5$ (GST), to enable phase change storage technology.[13]

Many technologically useful phase change materials are chalcogenides, which owe their success in this regard to a unique combination of properties, which include strong optical and electrical contrast, fast crystallization, and high crystallization temperature (typically several hundred degrees Celsius). **Figure 1** shows the ternary phase diagram of the Ge-Sb-Te system. As mentioned previously, alloys along the pseudo-binary line between Sb_2Te_3 and GeTe with compositions $(GeTe)_m(Sb_2Te_3)_n$ have been intensely studied[14] and are used in state-of-the-art PCM devices.[15] In search of

Simone Raoux, Institute Nanospectroscopy for Energy Material Design and Optimization, Helmholtz-Zentrum Berlin für Materialien und Energie GmbH, Germany; simone.raoux@helmholtz-berlin.de
Feng Xiong, Electrical Engineering, Stanford University, USA; fxiong@stanford.edu
Matthias Wuttig, Physikalisches Institut and Jülich Aachen Research Alliance – Fundamentals of Future Information Technology, RWTH Aachen University, Germany; wuttig@physik.rwth-aachen.de
Eric Pop, Electrical Engineering, Stanford University, USA; epop@stanford.edu
DOI: 10.1557/mrs.2014.139

© 2014 Materials Research Society

https://doi.org/10.1557/mrs.2014.139 Published online by Cambridge University Press

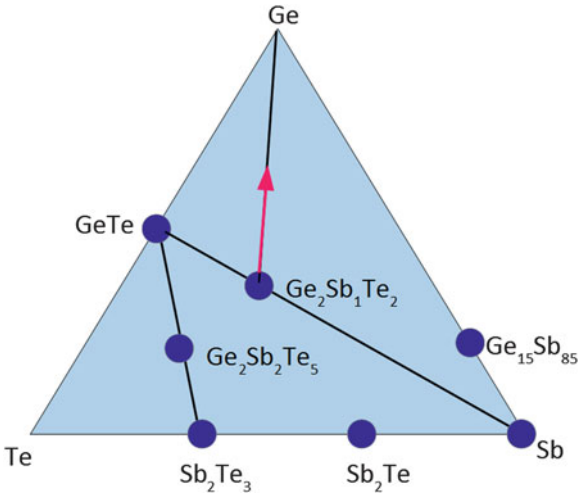


Figure 1. Tertiary Ge-Sb-Te phase diagram with some popular phase change alloys highlighted. The red arrow indicates the trend of adding Ge to $Ge_2Sb_1Te_2$ alloys.[19]

faster materials, undoped[16] and slightly Ge-doped Sb devices with a composition of $Ge_{15}Sb_{85}$[17] have been fabricated. The term "doping" is used in the phase change materials community to describe adding amounts of another element in the several percent range, but alloying would be a more accurate term. Another set of materials along the pseudo-binary line between GeTe and Sb was studied as well,[18] and starting from $Ge_2Sb_1Te_2$ on this line and the further addition of Ge (red arrow in Figure 1) led to the design of phase change materials with very high thermal stability of the amorphous phase, suitable for high-temperature PCM applications.[19]

All of these materials utilize a remarkable bonding mechanism in the crystalline phase, termed resonance bonding by Linus Pauling, where a single half-filled p-band forms two bonds to its left and right neighbors.[20,21] This bonding mechanism only prevails for a small subset of group V and VI compounds, which helps to identify and optimize possible phase change materials,[22] as illustrated in **Figure 2**. Resonance bonding requires long range order, and amorphous materials only employ ordinary covalent bonding. Crystallization is hence accompanied by a change in the bonding mechanism. Understanding the microscopic mechanisms employed in crystallization is crucial to optimize the performance of PCM data storage. In recent years, it has become clear that phase change materials are bad glass formers[23] that exhibit the characteristic behavior of fragile liquids,[24,25] including a pronounced temperature dependence of the activation barrier for crystal growth. This ensures that the amorphous phase is stable for 10 years at about 100°C (a typical industry benchmark), while this state recrystallizes into the crystalline phase in less than 10 ns at elevated temperatures around 500°C.[26,27] In fact, the fastest switching speeds reported are less than 1 ns.[28]

Principles of phase change memory

PCM is based on the repeated switching of a phase change material between the amorphous and the crystalline states associated with a large change in resistance. Information is stored in the phase of the material and is read by measuring the resistance of the PCM cell; the cell is programmed and read using electrical pulses. **Figure 3** illustrates the principle. Switching from the high-resistance or "reset" state, where part or all of the phase change material is amorphous, occurs when a current pulse is applied that heats the amorphous material above the crystallization temperature for a sufficiently long time for the material to crystallize. This is only possible because of the threshold switching effect that leads to a drastic and sudden (within nanoseconds) reduction of the resistance of the amorphous phase when a certain threshold field is surpassed, at a given threshold voltage V_T. Otherwise, it would be impossible to heat the amorphous material using Joule heating with reasonably low voltages. Switching from the low-resistance or "set" state, where the material is crystalline, is achieved by a high current pulse with a very short trailing edge. The current pulse heats the material by Joule heating, melts it, and enables very fast cooling (melt-quenching) such that the material solidifies in the amorphous state. The resistance state of the memory cell is read with a sufficiently small current pulse, which does not alter the state of the memory cell.

The previously mentioned threshold switching can be attributed to a current-voltage instability under a high electric field.[29] It does not necessarily lead to phase change, and if the high voltage is removed fast enough, the material will go back to the high resistance state. Threshold switching can be described as hot-electron trap-limited transport and a three-dimensional (3D) network model assuming a random distribution of traps.[30]

The current pulses are provided by an access device, which also isolates the memory cell during programming and read operations. Field-effect transistors,[31] bipolar junction transistors,[32] and diodes[33] have been used as access devices, and, in most cases, the size of the access device is larger than the PCM cell in order to provide sufficient current, ultimately limiting the storage density. Considerable development efforts have been devoted to optimizing the cell design that leads to reduced reset current, thus to reduced size of the access device and increased storage density.

Phase change materials are at the heart of PCM technology, and their properties to a large extent determine its functionality and success. Optimization of phase change materials is not only application specific but also technology node specific; for example, the threshold voltage in current typical PCM cells is on the order of 1 V, but if devices are scaled to much smaller dimensions, the threshold voltage scales with the size of the amorphous region, and for very small cells, it could become comparable to the read voltage such that every read operation could alter the cell state. In the following section, we discuss various possible PCM applications with their challenges and possible materials classes that could meet these challenges.

https://doi.org/10.1557/mrs.2014.139 Published online by Cambridge University Press

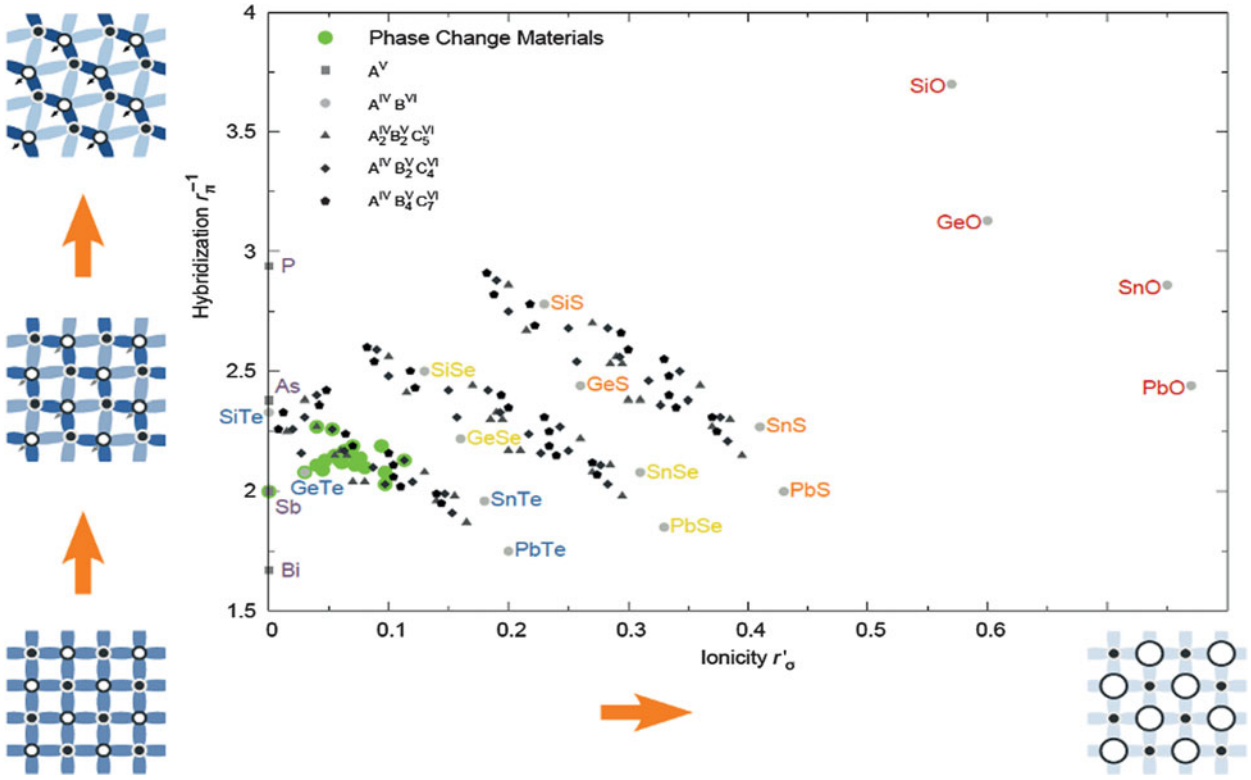


Figure 2. Empirical map for materials with about three *p*-electrons per atomic site and even numbers of anions and cations. The axes that span the map are the tendency toward hybridization, r_π^{-1}, and the ionicity, r'_σ. The coordinate r_π^{-1} describes the degree of covalency or tendency toward hybridization. It can be understood as a measure of the energetic splitting of *s*- and *p*-states, which scales with the difference between the radii of *s*- and *p*-orbitals. The coordinate r'_σ provides a quantitative measure for the ionicity of bonds similar to Pauling's electronegativity difference. The coordinates of a large number of materials have been calculated (see the supplement to Reference 22 for an index of materials). Different symbols in the map characterize different stoichiometry, where the subscript describes the stoichiometry, and the superscript identifies the formal valence of the corresponding atoms. Hence IV denotes atoms of group 14, while V and VI describe atoms of groups 15 and 16, respectively. Phase change materials are located within a small region of the map that is prone to the occurrence of resonant bonding. The graphics on the outside illustrate the weakening of resonance effects as one leaves this region due to the formation of more saturated covalent bonds via distortions or due to charge localization at the ions due to increasing ionicity. The size of the white and black circles is a measure of the electronegativity of the corresponding atoms. The different shades of blue represent different degrees of increasing electron localization. Reproduced with permission from Reference 22. © 2008 Nature Publishing Group.

The first application, which is already available in the market, is as stand-alone data storage to replace flash memory.[34] The requirements are moderate in terms of operation temperature (80°C), cycle number (10^5), and switching speed (ms range), and $Ge_2Sb_2Te_5$-based alloys can provide the required materials properties and switch at much faster times in the tens of ns range. For storage class memory applications such as a high-speed replacement for hard drives,[35] the requirements are higher, in particular in terms of the cycle numbers (10^8–10^9). New materials, such as reactively sputtered and doped $Ge_2Sb_2Te_5$, have been developed to increase the cycle numbers to 10^9 while maintaining fast switching (20 ns).[36] Due to the highly competitive nature of materials development for PCM, exact material compositions are often not published.

The requirements for data retention at higher temperatures are much more stringent for automotive applications (150°C for 10 years) or pre-coded chips that need to pass a solder bonding process (250–260°C for tens of seconds). In these cases, phase change materials with much higher crystallization temperatures compared to $Ge_2Sb_2Te_5$-based alloys are required. Highly Ge-rich Ge-Sb-Te materials, sometimes doped additionally with N and C, and GaSb have been shown to be promising candidates for these applications.[19,37,38]

Using PCM to replace DRAM is a formidable challenge, because very fast switching times in the nanoseconds range and extremely high cycle numbers of ~10^{16} present a combination of requirements that have not been achieved by phase change materials. DRAM replacement is a special case since DRAM is a volatile memory, whereas PCM is a non-volatile memory. If PCM were to achieve DRAM-like performance, it would open up possibilities to realize completely new computer architectures. Very fast switching times have been achieved for several phase change materials, including $Ge_2Sb_2Te_5$[27,28] and GeTe[26] in actual PCM devices. The high cycle number remains an enormous challenge, but it appears that scaling to smaller dimensions of the phase change material is beneficial

https://doi.org/10.1557/mrs.2014.139 Published online by Cambridge University Press

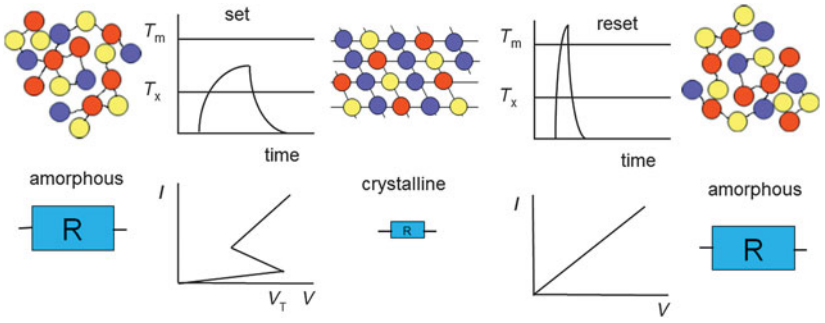


Figure 3. Principle of phase change memory. Starting from the amorphous phase with large resistance R, a current pulse is applied. At the threshold voltage V_T, the resistance drops suddenly, and a large current (I) flows that heats the material above the crystallization temperature T_x for a sufficiently long time to crystallize (set operation). In the crystalline state, the resistance is low. A larger, short current pulse is applied to heat the material above the melting temperature T_m. The material is melt-quenched and returns to the amorphous, high resistance state (reset operation). In the schematic, different colors represent different atoms (such as Ge, Sb, and Te in the commonly used GeSbTe compounds) in the phase change materials.

for cycling. Data measured on highly scaled PCM cells using an Sb-rich Ge-Sb-Te phase change material demonstrated 10^{11} cycles under accelerated testing conditions using a switching power of 45 pJ, which leads to an extrapolated cycle number of 6.5×10^{15} cycles under normal switching conditions using 3.6 pJ,[39] see **Figure 4**. Elemental segregation upon repeated cycling is one failure mechanism for PCM cells, and the ultra-scaled volume, which is likely completely molten in every reset operation, probably "remixes" the elements at every switching and also leaves very little room for the elements to spatially segregate, avoiding a typical failure mechanism.[40]

Phase change memory devices and integration

PCM will be successful in the market when it is possible to develop a manufacturing process that can achieve low cost and reliable production of large arrays of PCM cells and is compatible and easily incorporated in existing CMOS (complementary metal oxide semiconductor) processes. Device design and integration determine the PCM functionality and production costs, which are particularly important for PCM technology, and determine the size of the access device, which in turn determines the storage density.

The functionality of the PCM cell is strongly influenced by the choice of the phase change material, and large research efforts are devoted to optimizing phase change materials for specific applications with variable requirements for memory functionality such as switching speed, data retention, endurance, and switching power. The main failure mechanisms of PCM devices include the case where the cell can no longer be switched to the low resistance state, due to void formation over the bottom electrode contact, and is related to the change in mass density with the phase transformation and thus with every switching cycle. The other main failure mechanism is elemental segregation, in particular Sb enrichment in the switching region caused by electromigration. This leads to poor data retention when the cell can no longer be switched to the high resistance state or does not remain in the high resistance state since Sb-rich alloys have low crystallization temperatures.

A second important aspect is the cell design, which needs to consider many aspects such as number of required process steps, parameter window for each process step, availability of the required deposition methods (e.g., atomic layer deposition of phase change materials), and other aspects of manufacturability. Among the greatest challenges in PCM integration remains the reduction of the reset current. More details can be found in Chapter 17 of Reference 13.

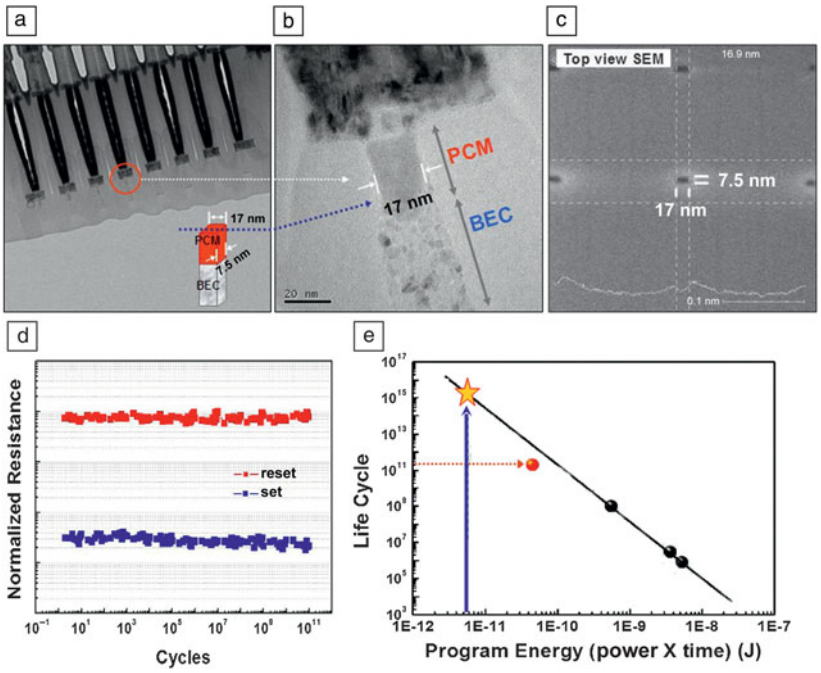


Figure 4. (a) Cross-sectional view transmission electron microscope (TEM) image of 7.5 nm (width) by 17 nm (length) dash confined phase change memory (PCM) cell, where the minimum size is defined by thin-film thickness rather than photolithography: (a) Lengthwise cross-section of eight devices. (b) Enlarged view of one device showing phase change film deposited by atomic layer deposition in contact with the bottom electrode contact (BEC). (c) Top view scanning electron microscope (SEM) cross-section of the bit. (d) Endurance characteristics (switching the cell back and forth between set and reset states) of dash confined cell at 4.5×10^{-11} J reset programming energy, marked in red in (e) where cycles to failure as a function of programming energy at acceleration condition are shown. The blue arrow indicates normal (not accelerated) program energy leading to an estimated cycle number of about 10^{15} (yellow star). Reprinted with permission from Reference 39. © 2010 IEEE.

https://doi.org/10.1557/mrs.2014.139 Published online by Cambridge University Press

Scaling properties of phase change materials and phase change memory

For PCM (or any new memory technology) to be viewed as a useful technology, it must demonstrate scalability for at least several generations to justify the heavy investment the industry needs to commit. Many efforts have been directed toward investigating PCM scalability at both the material and device level.

Table I shows a list of important parameters in phase change materials, their influence on PCM device performance, and how they behave when the material is scaled down to smaller dimensions. The crystallization temperature T_x of phase change materials can vary as a function of the material dimensions.[41–44] For instance, experiments performed on nm-thin films[45,46] and nanoparticles[47,48] suggest that T_x of phase change materials could increase under certain conditions with decreased dimensions. A higher T_x means that unintentional crystallization is less likely, and thus a longer data retention time prevails. T_x becomes a strong function of the interfaces for very thin films, and experiments on very thin Ge-Sb phase change films with various interface materials demonstrate that an increase or decrease of T_x can be observed, depending on the interface material, and the difference can be as large as 200°C for very thins films.[49] Measurements on $Ge_2Sb_2Te_5$ nanowire devices by Lee et al.[50] found that nanowires with smaller diameters have smaller activation energy, indicating a shorter data retention time. However, Yu et al.[51] did not observe a dependence of T_x on nanowire diameter. It has also been demonstrated that ultrathin films (1.3 nm thickness)[46] and tiny nanoparticles (2 nm diameter)[41] could still transform to the crystalline phase. *Ab initio* simulations have suggested that GeTe films could be scaled down to ~3.8 nm thickness (12 atomic layers), although in thinner films, overlapping metal-induced gap states from the two TiN electrodes could lead to a decrease in the on-off ratio.[52] The melting temperature T_m of phase change materials has also been observed to decrease with reduced dimensions in thin films,[40] nanowires,[53] and nanoparticles.[54] A lower T_m is generally favorable, implying that less power would be needed in the power-limiting reset step. Taken together, these experimental and theoretical results suggest good potential for scaling down PCMs, which is promising for future generations.

The crystallization speed of the phase change materials either increases (desirable) or decreases (detrimental) at reduced dimensions, depending on the material composition.[10,55] The thermal conductivity of phase change materials in both amorphous and crystalline phases is important and should be quite small, because it determines how energy-efficient the PCM device is during programming. Reifenberg et al.[56] studied the thermal conductivity of $Ge_2Sb_2Te_5$ thin films (60 nm and 350 nm) in the amorphous, face-centered cubic, and hexagonal states. They found that the thermal conductivity decreases as the film thickness decreases in all three phases. This suggests a favorable scaling trend since it helps reduce thermal power loss during operations.

The threshold voltage is found to show a linear relationship with the device dimension, suggesting an underlying threshold electric field.[16] This is beneficial for scaling down of voltage and power, although contact resistance effects may become dominant for the smallest devices.[57] The resistivity ratio of phase change materials does not appear to decrease in experiments on nanoscale devices,[58,59] although simulations mentioned previously predict such effects may occur at dimensions below a dozen atomic layers.[52] This means there would be a large enough window for multi-level cell programming in PCM even at diminished dimensions.[60] Overall, phase change materials demonstrate a highly desirable scaling behavior, which can be extended to several generations of technology nodes.

One of the major considerations of prototype PCM devices is their programming current, which can be large during the power-intensive reset step.[17] One approach to decrease the reset current (I_{reset}) is to reduce the volume of the phase change region, thus requiring lower overall power to heat up and reset it. This can be done by reducing the contact area between the phase change material and the electrodes. **Figure 5** shows I_{reset} as a function of the effective contact area for different cell structures.[39,58,59,61–64] It is evident that I_{reset} scales with the effective contact area, indicating an average reset current density of ~40 MA/cm^2. Thus, by using sub-lithographic scale electrodes, such as carbon nanotubes with diameters of a few nanometers, the reset current could be reduced to as low as a few μA.[58,59,65] At the same time, innovative device design by optimizing the thermal control could reduce the current density even further. For example, a larger thermal boundary resistance (TBR) between the PCM bit and its surrounding materials would act as a thermal insulation layer, retaining heat within the PCM volume and thus requiring lower reset current.[66] Such a demonstration was achieved by increasing the TBR with a thin layer of fullerenes (C_{60}) inserted between the phase change material and the metal electrode.[67] These promising results provide directions on how to overcome high reset currents, which are arguably one of the greatest obstacles in PCM technology.

We also briefly discuss the minimum amount of energy required to melt and reset a PCM bit from a thermodynamic perspective.

Table I. Scaling of phase change memory properties.

Material Property	Influence on Phase Change Memory Device	Scaling Behavior
Crystallization temperature T_x	Set power	Good
Melting temperature T_m	Reset power	Good
Crystallization speed	Data rate and set power	Depends
Thermal conductivity (amorphous and crystalline)	Set and reset power	Good
Threshold voltage	Set voltage/power	Good

https://doi.org/10.1557/mrs.2014.139 Published online by Cambridge University Press

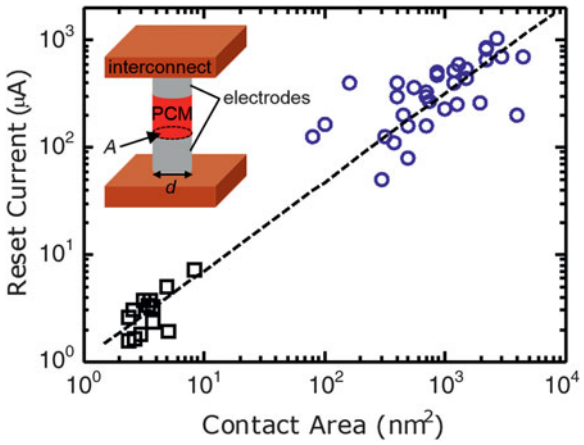


Figure 5. Reset current scaling versus electrode contact area in phase change memory (PCM) devices. The inset shows a schematic of a typical PCM cell, where *A* is the contact area and *d* is the contact diameter. Blue circles represent devices with metal contact electrodes (typically TiN), which are lithographically defined.[39,61–64] The black squares are data taken on prototype devices with carbon nanotube (CNT) electrodes.[58,59] The single- and multi-wall CNTs have diameters of the order of a few nm, contacting PCM bits with volumes of a few hundred nm^3. Updated and reprinted with permission from Reference 59. © 2013 American Chemical Society.

Assuming perfect thermal insulation of the bit (adiabatic heating), the energy for the reset step is the sum of the energy needed to heat up the crystalline bit from room temperature up to melting, plus the latent energy of the melting process. Taking the standard $Ge_2Sb_2Te_5$ (GST) properties,[68] (i.e., melting temperature $T_m \approx 600°C$, specific heat $C_s \approx 1.25$ J/cm^3/K, and latent heat of melting $H \approx 419$ J/cm^3), we estimate the minimum reset energy is $E_{min} = 1.2$ aJ/nm^3, which represents a fundamental lower limit for nanoscale PCM based on GST. In other words, a 5 × 5 × 5 nm^3 GST bit volume with perfect thermal insulation would require a minimum reset energy of approximately 150 aJ. A similar estimate based on the scaling of the bit contact area is given in Reference 69.

New applications of phase change memory

PCM cells cannot only be programmed in the on- or off-state, it is also possible to reach intermediate resistance states. Up to 16 levels have been demonstrated using a write-and-verify scheme.[60] Utilizing a continuous transition between resistance levels in PCM devices in an analog manner, this effect can be used to program them to mimic the behavior of a synapse, for example. Such an attempt could lead to the design of a neuromorphic computer with electronic hardware that resembles the functions of brain elements, such as the neurons and synapses. The phenomenon of spike-timing-dependent plasticity (a biological process where the strength of connections between neurons are adjusted during learning) could be demonstrated in PCM devices using specific programming schemes.[67,70] Image recognition using a neural network of PCM devices was also demonstrated.[71–73] These could potentially lead to a compact and low power neuromorphic computing system that is capable of processing information through learning, adaptation, and probabilistic association like the brain.

The thermoelectric (TE) effect, which corresponds to the conversion of thermal energy into electrical energy, has also been actively studied in the context of PCM materials and devices.[74,75] TE efficiency is characterized by the figure of merit $ZT = \sigma S^2 T/k$, where σ is the electrical conductivity, k is the thermal conductivity, T is the temperature, and S is the Seebeck coefficient. Phase change materials have good properties as *p*-type TEs because they have similar chemical compositions compared to traditional telluride-based TE materials, along with low thermal conductivity and relatively high electrical conductivity, which improves ZT. Chalcogenide-based phase change materials have been shown to exhibit $S \sim 350–380$ μVK^{-1} [76,77] and $ZT \sim 0.7$ at elevated temperatures[78] (commercial TE materials have $ZT \sim 1$). This opens up opportunities for applications such as Peltier coolers (heat $Q = IT\Delta S$ is removed at a junction of materials with different S as electric current I flows through) or power generators based on phase change materials. Studies have also suggested that both the Thomson effect (heating or cooling in a homogeneous material with a temperature gradient and T-dependent Seebeck coefficient) within PCM cells and the Peltier effect at the PCM electrode contacts could be used to control device heating, and thus reduce the reset current.[77,79] This effect is more prominent at smaller dimensions due to better thermal insulation. Thus, understanding and optimizing such TE phenomena could have a significant impact on future PCM device performance.

Summary

Phase change memory (PCM) is a promising novel data storage concept because of its unique combination of features such as fast access time, large electrical contrast, non-volatility, and high scalability. This article summarizes the properties and working principles of phase change materials, their applications to PCM devices, and how scaling affects these properties. The breakthrough discovery of fast switching materials along the pseudo-binary line between GeTe and Sb_2Te_3 has motivated researchers to further optimize material properties to improve the performance of PCM devices. Depending on the specific application, the requirements for important properties such as crystallization speed, thermal stability, and endurance are different. Material composition and preparation methods must be carefully optimized to meet the prerequisites of the specific application.

We also examined the scaling properties of phase change materials. Crystallization and melting temperature, crystallization speed, and thermal and electrical resistivity tend to demonstrate favorable scaling behavior when device dimensions are reduced to the nanometer range. PCM endurance could improve to 6.5 × 10^{15} cycles at ultra-scaled dimensions since complete melting of the bit would eliminate elemental segregation, which is a typical failure mechanism for PCM cells.

https://doi.org/10.1557/mrs.2014.139 Published online by Cambridge University Press

Recent results have also shown that the reset current and operating power of PCM devices scale down with the electrode contact area, also leading to a reduction of the access device size (which needs to carry less current) and enhancing the overall storage density.

Acknowledgments

M.W. gratefully acknowledges funding within SFB 917 ("Nanoswitches") and by the ERC ("Disorder Control"). F.X. and E.P. acknowledge support from the US National Science Foundation (NSF) grant ECCS 1002026 and from the US Office of Naval Research (ONR) grant N00014–10–1–0853.

References

1. W.J. Gallagher, S.S.P. Parkin, *IBM J. Res. Dev.* **50**, 5 (2006).
2. T. Kawahara, K. Ito, R. Takemura, H. Ohno, *Microelectron. Reliab.* **52**, 613 (2012).
3. S.S.P. Parkin, M. Hayashi, L. Thomas, *Science* **320**, 190 (2008).
4. H. Ishiwara, M. Okuyama, Y. Arimoto, *Ferroelectric Random Access Memories: Fundamentals and Applications* (Springer, New York, 2004).
5. R. Waser, R. Dittmann, G. Staikov, K. Szot, *Adv. Mater.* **21**, 2632 (2009).
6. D.B. Strukov, G.S. Snyder, D.R. Steward, R.S. Williams, *Nature* **453**, 80 (2008).
7. M. Kund, G. Beitel, C.-U. Pinnow, T. Röhr, J. Schumann, R. Symanczyk, K.-D. Ufert, G. Müller, *IEEE Int. Electron Dev. Mtg.* 754 (Washington, DC, 2005).
8. T. Rueckes, K. Kim, E. Joselevich, G.Y. Tseng, C.-L. Cheung, C.M. Lieber, *Science* **7**, 94 (2000).
9. J.B. Cui, R. Sordan, M. Burghard, K. Kern, *Appl. Phys. Lett.* **81**, 3260 (2002).
10. S. Raoux, G.W. Burr, M.J. Breitwisch, C.T. Rettner, Y.-C. Chen, R.M. Shelby, M. Salinga, D. Krebs, S.-H. Chen, H.-L. Lung, C.H. Lam, *IBM J. Res. Dev.* **52**, 465 (2008).
11. S.R. Ovshinsky, *Phys. Rev. Lett.* **22**, 1450 (1968).
12. N. Yamada, E. Ohno, N. Akahira, K. Nishiuchi, K. Nagata, *Jpn. J. Appl. Phys.* **26** (Suppl. 26–4), 61 (1987).
13. S. Raoux, M. Wuttig, *Phase Change Materials: Science and Application* (Springer, New York, 2009).
14. J.L.F.D. Silva, A. Walsh, H.L. Lee, *Phys. Rev. B: Condens. Matter* **78**, 224111 (2008).
15. G. Servalli, *IEEE Int. Electron Dev. Mtg.* 113 (Washington, DC, 2009).
16. D. Krebs, S. Raoux, C.T. Rettner, G.W. Burr, M. Salinga, M. Wuttig, *Appl. Phys. Lett.* **95**, 082101 (2009).
17. Y.C. Chen, C.T. Rettner, S. Raoux, G.W. Burr, S.H. Chen, R.M. Shelby, M. Salinga, W. Risk, T.D. Happ, G.M. McClelland, M. Breitwisch, A. Schrott, J.B. Philipp, M.H. Lee, R. Cheek, T. Nirschl, M. Lamorey, C.F. Chen, E. Joseph, S. Zaidi, B. Yee, H.L. Lung, R. Bergmann, C. Lam, *IEEE Int. Electron Dev. Mtg.* 777 (San Francisco, CA, 2006).
18. H.-Y. Cheng, S. Raoux, J.L. Jordan-Sweet, *J. Appl. Phys.* **115**, 093101 (2014).
19. H.-Y. Cheng, T.H. Hsu, S. Raoux, J.Y. Wu, P.Y. Du, M. Breitwisch, Y. Zhu, E.K. Lai, E. Joseph, S. Mittal, R. Cheek, A. Schrott, S.C. Lai, H.L. Lung, C. Lam, *IEEE Int. Electron Dev. Mtg.* 3.4.1 (Washington, DC, 2011).
20. L. Pauling, *The Nature of the Chemical Bond* (Cornell University Press, New York, 1939).
21. K. Shportko, S. Kremers, M. Woda, D. Lencer, J. Robertson, M. Wuttig, *Nat. Mater.* **7**, 653 (2008).
22. D. Lencer, M. Salinga, B. Grabowski, T. Hickel, J. Neugebauer, M. Wuttig, *Nat. Mater.* **7**, 972 (2008).
23. J. Kalb, M. Wuttig, F. Spaepen, *J. Mater. Res.* **22**, 748 (2007).
24. J. Orava, A.L. Greer, B. Gholipour, D.W. Hewak, C.E. Smith, *Nat. Mater.* **11**, 279 (2012).
25. M. Salinga, E. Carria, A. Kaldenbach, M. Börnhöfft, J. Benke, J. Mayer, M. Wuttig, *Nat. Commun.* **4**, 2371 (2013).
26. G. Bruns, P. Merkelbach, C. Schlockermann, M. Salinga, M. Wuttig, T.D. Happ, J.B. Philipp, M. Kund, *Appl. Phys. Lett.* **95**, 043108 (2009).
27. W.J. Wang, L.P. Shi, R. Zhao, K.G. Lim, H.K. Lee, T.C. Chong, Y.H. Wu, *Appl. Phys. Lett.* **93**, 043121 (2008).
28. D. Loke, T.H. Lee, W.J. Wang, L.P. Shi, R. Zhao, Y.C. Yeo, T.C. Chong, S.R. Elliott, *Science* **336**, 1566 (2012).
29. D. Ielmini, Y. Zhang, *J. Appl. Phys.* **102**, 054517 (2007).
30. A. Capelli, E. Piccinini, F. Xiong, A. Behnam, R. Brunetti, M. Rudan, E. Pop, C. Jacoboni, *Appl. Phys. Lett.* **103**, 083503 (2013).
31. S. Tyson, G. Wicker, T. Lowrey, S. Hudgens, K. Hunt, *Proc. IEEE Aerosp. Conf.* **5**, 385 (2000).
32. S.L. Cho, J.H. Yi, Y.H. Ha, B.J. Kuh, C.M. Lee, J.H. Park, S.D. Nam, H. Horii, B.O. Cho, K.C. Ryoo, S.O. Park, H.S. Kim, U.I. Chung, J.T. Moon, B.I. Ryu, *Symp. VLSI Technol.* 96 (2005).
33. M. Breitwisch, T. Nirschl, C.F. Chen, Y. Zhu, M.H. Lee, M. Lamorey, G.W. Burr, E. Joseph, A. Schrott, J.B. Philipp, R. Cheek, T.D. Happ, S.H. Chen, S. Zaidi, P. Flaitz, J. Bruley, R. Dasaka, B. Rajendran, S. Rossnagel, M. Yang, Y.C. Chen, R. Bergmann, H.L. Lung, C. Lam, *Symp. VLSI Technol.* 6B-3 (2007).
34. P. Pavan, R. Bez, P. Olivo, E. Zanoni, *Proc. IEEE* **85**, 1248 (1997).
35. G.W. Burr, B.N. Kurdi, J.C. Scott, C.H. Lam, K. Gopalakrishnan, R.S. Shenoy, *IBM J. Res. Dev.* **52**, 449 (2008).
36. H.Y. Cheng, M. BrightSky, S. Raoux, C.F. Chen, P.Y. Du, J.Y. Wu, Y.Y. Lin, T.H. Hsu, Y. Zhu, S. Kim, H.L. Lung, C. Lam, *IEEE Int. Electron Dev. Mtg.* 30.6.1 (Washington, DC, 2013).
37. G. Navarro, M. Coue, A. Kiouseloglou, P. Noe, F. Fillot, V. Delaye, A. Persico, A. Roulle, M. Bernard, C. Sabbione, D. Blanchier, V. Sousa, L. Perniola, S. Maitrejean, A. Cabrini, G. Torelli, P. Zuliani, R. Annunziata, E. Palumbo, M. Borghi, G. Reimbold, B. De Salvo, *IEEE Int. Electron Dev. Mtg.* 21.5.1 (Washington, DC, 2013).
38. H.-Y. Cheng, S. Raoux, K.V. Nguyen, R.S. Shenoy, M. BrightSky, *Appl. Phys. Lett.* in press (2014).
39. I.S. Kim, S.L. Cho, D.H. Im, E.H. Cho, D.H. Kim, G.H. Oh, D.H. Ahn, S.O. Park, S.W. Nam, J.T. Moon, C.H. Chung, *Symp VLSI Technol.* **203** (2010).
40. S. Raoux, R.M. Shelby, J. Jordan-Sweet, B. Munoz, M. Salinga, Y.-C. Chen, Y.-H. Shih, E.-K. Lai, M.-H. Lee, *Microelectron. Eng.* **85**, 2330 (2008).
41. M.A. Caldwell, S. Rauox, R.Y. Wang, H.-S.P. Wong, D.J. Milliron, *J. Mater. Chem.* **20**, 1285 (2010).
42. H.F. Hamann, M. O'Boyle, Y.C. Martin, M. Rooks, K. Wickramasinghe, *Nat. Mater.* **5**, 383 (2006).
43. H. Satoh, K. Sugawara, K. Tanaka, *J. Appl. Phys.* **99**, 2 (2006).
44. F. Xiong, A. Liao, E. Pop, *Appl. Phys. Lett.* **95**, 243103 (2009).
45. T. Gotoh, K. Sugawara, K. Tanaka, *J. Appl. Phys.* **43**, L818 (2004).
46. S. Raoux, J.L. Jordan-Sweet, A.J. Kellock, *J. Appl. Phys.* **103**, 114310 (2008).
47. D.S. Suh, E. Lee, K.H.P. Kim, J.S. Noh, W.C. Shin, Y.S. Kang, C. Kim, Y. Khang, H.R. Yoon, W. Jo, *Appl. Phys. Lett.* **90**, 2 (2007).
48. H.S. Choi, K.S. Seol, K. Takeuchi, J. Fujita, Y. Ohki, *J. Appl. Phys.* **44**, 7720 (2005).
49. S. Raoux, H.-Y. Cheng, J.L. Jordan-Sweet, B. Munoz, M. Hitzbleck, *Appl. Phys. Lett.* **94**, 183144 (2009).
50. S.H. Lee, D.K. Ko, Y. Jung, R. Agarwal, *Appl. Phys. Lett.* **89**, 22 (2006).
51. D. Yu, S. Brittman, J.S. Lee, A.L. Falk, H. Park, *Nano Lett.* **8**, 3429 (2008).
52. J. Liu, M.P. Anantram, *J. Appl. Phys.* **113**, 063711 (2013).
53. X.H. Sun, B. Yu, G. Ng, T.D. Nguyen, M. Meyyappan, *Appl. Phys. Lett.* **89**, 23 (2006).
54. X.H. Sun, B. Yu, G. Ng, M. Meyyappan, *J. Phys. Chem. C* **111**, 2421 (2007).
55. G.W. Burr, M.J. Breitwisch, M. Franceschini, D. Garetto, K. Gopalakrishnan, B. Jackson, B. Kurdi, C. Lam, L.A. Lastras, A. Padilla, B. Rajendran, S. Raoux, R.S. Shenoy, *J. Vac. Sci. Technol. B* **28**, 223 (2010).
56. J.P. Reifenberg, M.A. Panzer, S. Kim, A.M. Gibby, Y. Zhang, S. Wong, H.-S. P. Wong, E. Pop, K.E. Goodson, *Appl. Phys. Lett.* **91**, 111904 (2007).
57. D. Roy, M.A.A. Zandt, R.A.M. Wolters, *IEEE Electron Devices Lett.* **31**, 1293 (2010).
58. F. Xiong, A.D. Liao, D. Estrada, E. Pop, *Science* **332**, 568 (2011).
59. F. Xiong, M.H. Bae, Y. Dai, A.D. Liao, A. Behnam, E.A. Carrion, S. Hong, D. Ielmini, E. Pop, *Nano Lett.* **13**, 464 (2013).
60. T. Nirschl, J.B. Philipp, T.D. Happ, G.W. Burr, B. Rajendran, M.-H. Lee, A. Schrott, M. Yang, M. Breitwisch, C.-F. Chen, E. Joseph, M. Lamorey, R. Cheek, S.-H. Chen, S. Zaidi, S. Raoux, Y.C. Chen, Y. Zhu, R. Bergmann, H.-L. Lung, C. Lam, *IEEE Int. Electron Dev. Mtg.* 461 (Washington, DC, 2007).
61. A. Pirovano, A.L. Lacaita, A. Benvenuti, F. Pellizzer, S. Hudgens, R. Bez, *IEEE Int. Electron Dev. Mtg.* 699 (Washington, DC, 2003).
62. D.H. Im, J.I. Lee, S.L. Cho, H.G. An, D.H. Kim, I.S. Kim, H. Park, D.H. Ahn, H. Horii, S.O. Park, U.-I. Chung, J.T. Moon, *IEEE Int. Electron Dev. Mtg.* 211 (San Francisco, CA, 2008).
63. M.J. Kang, T.J. Park, Y.W. Kwon, D.-H. Ahn, Y.S. Kang, H.-S. Jeong, S.-J. Ahn, Y.J. Song, B.C. Kim, S.-W. Nam, H.-K. Kang, G.-T. Jeong, C.-H. Chung, *IEEE Int. Electron Dev. Mtg. (IEDM)*, 39 (2011).
64. H.-S.P. Wong, S. Raoux, S.B. Kim, J. Liang, J.P. Reifenberg, B. Rajendran, M. Asheghi, K.E. Goodson, *Proc. IEEE* **98**, 2201 (2010).
65. J.L. Liang, R.G.D. Jeyasingh, H.Y. Chen, H.-S.P. Wong, *IEEE Trans. Electron Devices* **59**, 1155 (2012).
66. E. Bozorg-Grayeli, *Annu. Rev. Heat Transfer* **16**, 397 (2013).
67. C. Kim, D.-S. Suh, K.H.P. Kim, Y.-S. Kang, T.-Y. Lee, Y. Khang, D.G. Cahill, *Appl. Phys. Lett.* **92**, 013109 (2008).
68. A. Redaelli, A. Pirovano, A. Benvenuti, A.L. Lacaita, *J. Appl. Phys.* **103**, 111101 (2008).
69. A.L. Lacaita, A. Redaelli, *Microelectron. Eng.* **109**, 351 (2013).
70. B.L. Jackson, B. Rajendran, G.S. Corrado, M. Breitwisch, G.W. Burr, R. Cheek, K. Gopalakrishnan, S. Raoux, C.T. Rettner, A. Padilla, A.G. Schrott, R.S. Shenoy, B.N. Kurdi, C.H. Lam, D.S. Modha, *ACM J. Emerg. Technol.* **9**, 12 (2013).

https://doi.org/10.1557/mrs.2014.139 Published online by Cambridge University Press

71. M. Suri, O. Bichler, D. Querlioz, O. Cueto, L. Perniola, V. Sousa, D. Vuillaume, C. Gamrat, B. De Salvo, *IEEE Int. Electron Dev. Mtg.* 4.4.1 (Washington, DC, 2011).
72. D. Kuzum, R.G.D. Jeyasingh, B. Lee, H.-S.P. Wong, *Nano Lett.* **12**, 2179 (2012).
73. M. Suri, O. Bichler, D. Querlioz, B. Traor, O. Cueto, L. Perniola, V. Sousa, D. Vuillaume, C. Gamrat, B. De Salvo, *J. Appl. Phys.* **112**, 054904 (2012).
74. D.-S. Suh, C. Kim, K.H.P. Kim, Y.-S. Kang, T.-Y. Lee, Y. Khang, T.S. Park, Y.-G. Yoon, J. Im, J. Ihm, *Appl. Phys. Lett.* **96**, 123115 (2010).
75. T. Rosenthal, M.N. Schneider, C. Stiewe, D. Markus, O. Oeckler, *Chem. Mater.* **23**, 4349 (2011).
76. E. Bozorg-Grayeli, J.P. Reifenberg, M. Asheghi, H.-S.P. Wong, K.E. Goodson, *Annu. Rev. Heat Transfer* **15**, 1437 (2012).
77. K.L. Grosse, F. Xiong, S. Hong, W.P. King, E. Pop, *Appl. Phys. Lett.* **102**, 193503 (2013).
78. E.-R. Sittner, K.S. Siegert, P. Jost, C. Schlockermann, F.R. Lange, M. Wuttig, *Phys. Status Solidi* **210**, 147 (2013).
79. J. Lee, M. Asheghi, K.E. Goodson, *Nanotechnology* **23**, 205201 (2012). □

2015 MRS® SPRING MEETING & EXHIBIT
April 6–10, 2015 | San Francisco, California

CALL FOR PAPERS

Abstract Submission Opens September 23, 2014 | Abstract Submission Deadline October 23, 2014

Energy
A Emerging Silicon Science and Technology
B Thin-Film Compound Semiconductor Photovoltaics
C Perovskite Solar Cells
D Organic-Based Photovoltaics
E Advanced Solar Cells—Components to Systems
F Biohybrid Solar Cells—Photosynthesis-Based Photovoltaics and Photocatalytic Solar Cells
G Next-Generation Electrochemical Energy Storage and Conversion Systems—Synthesis, Processing, Characterization and Manufacturing
H Mechanics of Energy Storage and Conversion—Batteries, Thermoelectrics and Fuel Cells
I High Capacity Anode Materials for Lithium Ion Batteries
J Latest Advances in Solar Water Splitting
K The Development of Oxygen Reduction Reaction (ORR) and Oxygen Evolution Reaction (OER) Materials in Energy Storage and Conversion Systems

Nanomaterials
L Bioinspired Micro- and Nano-Machines—Challenges and Perspectives
M Nanoscale Heat Transport—From Fundamentals to Devices
N From Molecules to Colloidal Compound Semiconductor Nanocrystals—Advances in Mechanism-Enabled Design and Syntheses
O Emerging Non-Graphene 2D Materials
P Nanogenerators and Piezotronics
Q Externally Actuated Responsive Nanomaterials—Design, Synthesis, Applications and Challenges
R Photoactive Nanoparticles and Nanostructures
S Semiconductor Nanowires and Devices for Advanced Applications
T Graphene and Carbon Nanotubes

Electronics and Photonics
U The Interplay of Structure and Carrier Dynamics in Energy-Relevant Nanomaterials
V Resonant Optics—Fundamentals and Applications
W Light-Matter Processes in Molecular Systems and Devices
Y Phase-Change Materials for Data Storage, Cognitive Processing and Photonics Applications
Z Plasmonics and Metamaterials—Synthesis, Characterization and Integration
AA Materials for Beyond the Roadmap Devices in Logic, Power and Memory
BB Innovative Interconnects/Electrodes for Advanced Devices, Flexible and Green-Energy Electronics
CC Reliability and Materials Issues of Semiconductors—Optical and Electron Devices and Materials III
DD Tailored Disorder—Novel Materials for Advanced Optics and Photonics
EE Quantum Photonics, Information Technology and Sensing
FF Defects in Semiconductors—Relationship to Optoelectronic Properties

Soft and Biomaterials
GG Foundations of Bio/Nano Interfaces—Synthesis, Modeling, Design Principles and Applications
HH Supramolecular Materials—Assembly and Dynamics
II Organic Bioelectronics—Materials, Processes and Applications
JJ Exploiting Bioinspired Self-Assembly for the Design of Functional and Responsive Materials
KK Nanomaterials in Translational Medicine
LL Soft Electronics—From Electronic Skin to Reliable Neural Interfaces
MM Crystal Engineering—Design, New Materials and Applications

General—Fabrication and Characterization
NN Adaptive Architecture and Programmable Matter—Next-Generation Building Skins and Systems from Nano to Macro
OO Metal-Assisted Chemical Etching of Silicon and Other Semiconductors
PP Gold-Based Materials and Applications
QQ Plasma-Based Materials Science and Engineering
RR Solution Syntheses of Inorganic Functional/Multifunctional Materials
SS Oxide Thin Films and Nanostructures for Advanced Electrical, Optical and Magnetic Applications
TT Metal Oxides—From Advanced Fabrication and Interfaces to Energy and Sensing Applications
UU Titanium Oxides—From Fundamental Understanding to Applications
VV Science and Technology of Superconducting Materials
WW Ultrafast Dynamics in Complex Functional Materials
XX Multiscale Modeling and Experiments on Microstructural Evolution in Nuclear Materials
YY Insights for Energy Materials Using *In-Situ* Characterization
ZZ Materials Information Using Novel Techniques in Electron Microscopy

www.mrs.org/spring2015

Meeting Chairs
Artur Braun Swiss Federal Laboratories for Materials Science and Technology
Hongyou Fan Sandia National Laboratories
Ken Haenen Hasselt University and IMEC vzw
Lia Stanciu Purdue University
Jeremy A. Theil Quantumscape, Inc.

Don't Miss These Future MRS Meetings!
2015 MRS Fall Meeting & Exhibit
November 29 – December 4, 2015
Hynes Convention Center & Sheraton Boston Hotel
Boston, Massachusetts
2016 MRS Spring Meeting & Exhibit
March 28 – April 1, 2016
Phoenix Convention Center
Phoenix, Arizona

MRS MATERIALS RESEARCH SOCIETY®
Advancing materials. Improving the quality of life.
506 Keystone Drive • Warrendale, PA 15086-7573
Tel 724.779.3003 • Fax 724.779.8313
info@mrs.org • www.mrs.org

https://doi.org/10.1557/mrs.2014.139 Published online by Cambridge University Press